



DATASHEET

PrecisIOn™

rNav1.8-ND7

Recombinant Cell Line

CATALOG # CYL3050
REVISION # M07

ORDERING INFORMATION AND TECHNICAL SERVICES

Millipore (UK) Ltd
6-7 Technopark
Cambridge CB5 8PB
UK

Tel: +44 (0) 1223 508191
Fax: +44 (0) 1223 508198

CUSTOMER SERVICES

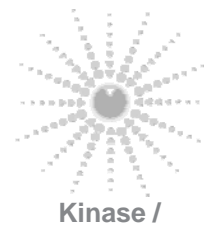
UK: 0800 0190 333
US: 800 437 7500



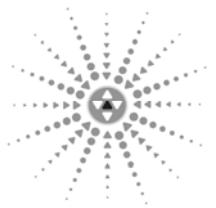
GPCR



Ion Channels



Kinase /
Phosphatase



Safety & Toxicity
Profiling

Product description:

Recombinant ND7-23 (rat DRG/mouse neuroblastoma hybrid) cell line expressing the rat Nav1.8 (type 10 voltage-gated sodium channel, alpha polypeptide (Scn10a), accession number U53833).

Format:

2 x 1 ml aliquots containing 1.08×10^6 cells/ml in 10% DMSO at passage 7 (lot 3).

Mycoplasma Testing:

The cell line has been screened using the MycoSensor™ PCR Assay Kit (Stratagene) to confirm the absence of Mycoplasma species.

Functional Validation:

ND7-23 cells expressing rNav1.8 were characterized in terms of their pharmacological and biophysical properties using whole-cell patch clamp techniques.

The cell line was shown to be expressing rNav1.8 currents since it was resistant to TTX (100 nM) but blocked by tetracaine in the micromolar range.

The currents also had biophysical properties similar to published data where Nav1.8 has been expressed in recombinant systems. For example they were activated at potentials more positive to -45 mV, the peak of I/V relationship was 0/+10 mV, $V_{1/2}$ of activation was -9 mV and $V_{1/2}$ of inactivation was around -50 mV.

Channel expression, monitored using IonWorks™ HT, is stable over at least 70 passages. Typically, for a given passage, over 80% of the cells express peak inward currents greater than 200 pA with a mean amplitude of between 500-600 pA.

This cell line is also suitable for voltage sensitive probe assays. Using such an assay, the sodium channel opener deltamethrin induced Na^+ -dependent membrane potential depolarizations with an EC_{50} of approximately 1 μM that were blocked by micromolar concentrations of tetracaine.

Recommended Culture Conditions:

Recommended culture conditions and standard operating procedure are provided with the product.

Licensing Statements

The CMV promoter is covered under U.S. Patents 5,168,062 and 5,385,839 and its use is permitted for research purposes only. Any other use of the CMV promoter requires a license from the University of Iowa Research Foundation, 214 Technology Innovation Center, Iowa City, IA 52242, USA.

The bovine growth hormone (bgh) polyadenylation signal and its use in the expression of recombinant proteins is covered by claims listed in U.S. Patent No. 5,122,458, EU Patent No. 0 173 552 and Japanese Patent No. 1955752 (collectively "CLAIMED DNA and/or CLAIMED CELLS") owned and licensed to Millipore (formerly Upstate Biotechnology Inc.) by Research Corporation Technologies, Inc., 101 North Wilmot Road, Suite 600, Tucson, AZ 85711-3335 ("RCT").

Use of this technology is restricted to research purposes only. The purchased/licensed cell line and all bacteria, phages and plasmids derived from this cell line, in whole or in part, and all proteins expressed from the cell line shall be used for research uses only. "Research purposes" means uses directed to the identification of useful recombinant proteins and the investigation of the recombinant expression of proteins. In no event shall research use include any of the following: any use in humans of a CLAIMED DNA or CLAIMED CELL; any use in human or protein expression or other substance expressed or made at any stage of its production that use the CLAIMED DNA or a CLAIMED CELL; or any use in which a CLAIMED DNA or CLAIMED CELL would be sold or transferred to a third party. No license, other than research use, is expressed or implied by the purchase/license of the cell line. By accepting or using Millipore's cell line product, you agree to be bound for the following use/license restrictions:

This product enables the user which purchased/licensed it to use the cDNA construct for research purposes only and additional restrictions apply to commercial uses of the cell line. Such commercial uses, include uses such as resale, bulk preparation of proteins encoding the cDNA, application of the product with transgenic animals or human experiments, or use in screening or drug development. All commercial uses require a separate written license from Millipore Corporation and may require additional licenses from RCT, whose contact is Dr. Jennifer Tonzello, phone, +001 520-748-4441.

IonWorks™ HT is a trademark of Molecular Devices Corporation

Electrophysiological Properties of the rNav1.8 Current.**Conventional Whole-Cell Patch Clamp Electrophysiology.**

Electrophysiological experiments were conducted at room temperature (20–22°C) on rNav1.8-ND7 23 cells up to 3 days after plating. As a comparison, experiments on rat DRG neurons of 10–25 µm somatic diameter were carried out within 1–36 h of plating. Cells were superfused with an extracellular solution at a rate of 2 ml/min. Patch pipettes were filled with internal recording solution to give final tip resistances of 2–4 mΩ. The following external (bath) and internal (pipette) solutions were used (mM in double dH₂O): DRG internal; CsF (110), HEPES (10), MgCl₂ (5), NaCl (10), pH7.25; DRG external; NaCl (60), HEPES-Na(10), MgCl₂ (5), KCl (5), Choline Cl (50), CaCl₂ (1), TEA (30), TTX (0.0001), pH7.4; HEK293 and ND7–23 Nav1.8 internal; CsF (120), HEPES (10), EGTA (10), NaCl (15), pH 7.25; HEK293 and ND7–23 Nav1.8 external; NaCl (140), HEPES-Na (5), MgCl₂ (1.3), CaCl₂ (1), Glucose (11), KCl (4.7), TTX (0.0001), pH7.4. External and internal solutions were adjusted to osmolarities of 295–300 and 285–290 mOsm respectively. Capacitance transients and series resistance errors were compensated for (80–85%) using the amplifier circuitry and linear leakage currents were subtracted using an on-line 'P/4' procedure provided by the commercial software package. Membrane potentials were corrected for liquid junction potentials off-line (+7 and +8 for DRG and recombinant cell conditions, respectively).

Data from conventional whole-cell patch clamp electrophysiology experiments are summarized in **Table 1**.

Table 1. Comparison of biophysical properties of the rNav1.8 cell line and rat DRG cells. Data were generated in the presence of 100 nM tetrodotoxin (TTX). All voltage-command protocols were conducted from a holding voltage of –90 mV. The slow inactivation protocol comprised a prepulse of 4 s (or 10 s) duration followed immediately by a test pulse to 0 mV. For the fast inactivation a prepulse of 15 ms was employed. Recovery from inactivation was assessed using a prepulse of 4 s to 0 mV followed by a recovery period and then a test pulse to 0 mV. Data are mean ± SEM (n = 4-12).

Current	Activation V _{1/2} (mV)	Activation <i>k</i> (mV/e-fold)	Activation TTP (ms)	Inactivation V _{1/2} (mV)	Inactivation <i>k</i> (mV/e-fold)	Inactivation τ (ms)	Recovery from inactivation τ (ms)
Nav1.8 ND7-23	-9.4±1.5	5.8±0.7	2.1±0.2	Slow -49.5±4.2	7.3±0.2	8.6±0.5	τ ₁ 12.5±1.6
				Fast -30.8±0.7	11.2±0.4		τ ₂ 2271±289
DRG TTXR	-17.2±2.9	7.0±0.5	1.5±0.3	Slow -54.1± 0.6	4.8±0.4	4.1±0.6	τ ₁ 22.2±9.9
				Fast -19.7± 2.0	6.0±1.0		τ ₂ 137±31

TTP = time to peak (ms). ND - not determined.

Current/Voltage Relationship:

Figure 1 shows representative rNav1.8 currents, evoked by 25 ms voltage steps from -80 mV to +30 mV in 10 mV increments, applied from a holding potential of -90 mV. Activation of the current occurred at potentials more positive to -45 mV (the reported range of threshold of activation is -30 to -50 mV (Dekker *et al*, 2005, Leffler *et al*, 2006 and Zhou *et al*, 2003) and the amplitude increased up to approximately 0/+10 mV (peak inward current) again in agreement with published findings (Dekker *et al*, 2005 and Zhou *et al*, 2003 (both +10 mV)). At more positive voltages the currents became smaller due to the onset of slow inactivation. The reversal potential (E_{rev}) was $+42 \pm 1$ mV, 14 mV less than the theoretical E_{Na} (+56 mV). In wild type ND7-23 cells, small outward, possibly Cs^+ currents were observed (in the presence of TTX) at positive potentials (>+20 mV) under our recording conditions, which may explain the difference between E_{rev} and theoretical E_{Na} in rNav1.8-ND7 23. The current/voltage relationship is plotted in **Figure 2**.

Figure 1. Expression of rNav1.8 in ND7-23 cells.

Representative current traces (upper panel) for a series of voltage steps from -90 mV (voltage protocol - lower panel).

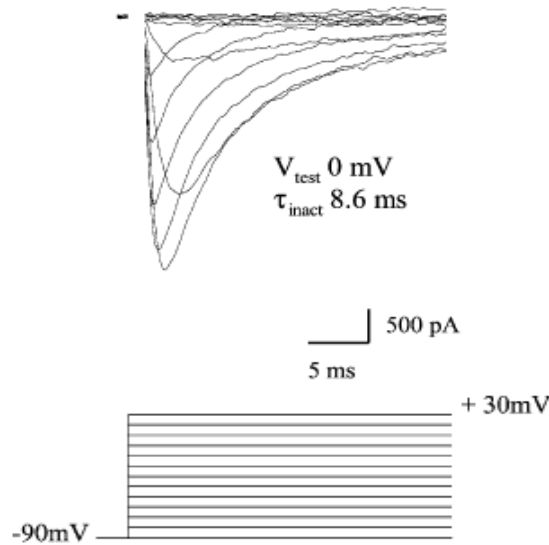
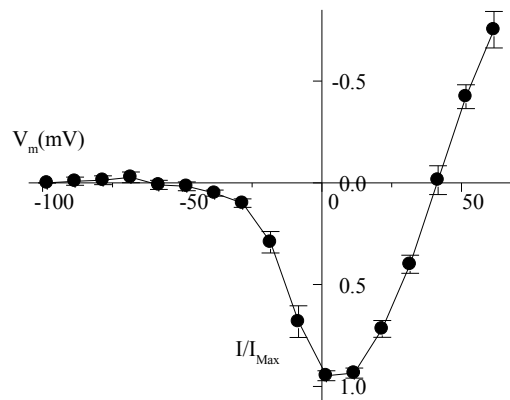


Figure 2. Current/Voltage relationship for rNav1.8 in ND7-23 cells.

The peak current at each test potential was normalized to the maximum current (I/I_{max}) obtained from a given cell (Data are mean \pm SEM, n=6).



Voltage-Dependence of Channel Activation and Inactivation:**Activation:**

Boltzmann analysis of rNav1.8 conductance (**Figure 3, Activation**) yielded a $V_{1/2}$ of -9.4 ± 1.5 mV ($n=11$), which is less negative than the value calculated for the TTX-resistant (TTX-R) current in DRG neurons (-17.2 ± 2.9 mV, $n=8$) but similar (-11 mV) to that obtained for a recombinantly expressed human Nav1.8 channel in SH-SY5Y cells (Dekker *et al* 2005). The slope value (k) was 5.8 ± 0.7 ($n=11$) for rNav1.8 compared to 7.0 ± 0.5 for DRG TTX-R.

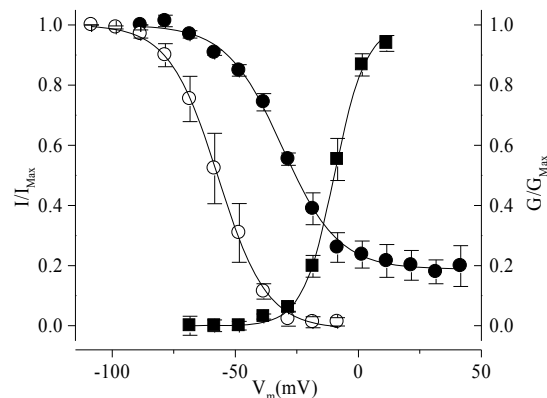
Inactivation:

The voltage-dependence of rNav1.8 inactivation was studied using a two-pulse voltage-clamp protocol that comprised a pre-pulse to various potentials between -120 and $+40$ mV, followed by a test pulse to 0 mV (the peak of the rNav1.8 current/voltage curve). Inactivation curves were constructed at two different prepulse durations; a 15 ms pre-pulse to measure fast inactivation and a 4 s pre-pulse to mimic 'steady-state' inactivation. With the shorter pre-pulse duration, a small, non-inactivating component (approximately 20%) was recorded (**Figure 3, Inactivation**). With the 4 s pre-pulse, the parameters describing the voltage-dependence of slow rNav1.8 inactivation were very similar for the rNav1.8-ND7 23 stable cell line and the TTX-resistant Na^+ current recorded in DRG neurons ($V_{1/2}$ -49.5 ± 4.2 and -54.1 ± 0.6 mV, respectively) and in line with published values (-34 ; Zhou *et al*, 2003 and -40 mV; Leffler *et al*, 2006). With a shorter 15 ms pre-pulse, significant differences were seen between rNav1.8 and DRG TTX-R current. The $V_{1/2}$ of fast inactivation in the rNav1.8 stable cell line was -30.8 ± 0.7 mV compared to -19.7 ± 2.0 mV for TTX-R.

Figure 3. Voltage-dependence of channel activation and inactivation.

Activation: The filled squares (■) show the normalized Boltzmann function for conductance (G/G_{max}) derived from the equation; $G/G_{\text{max}} = 1/[1 + \exp(V_{1/2} - V/k)]$ where G is the measured conductance, G_{max} is the maximal conductance, $V_{1/2}$ is the membrane potential at which the half-maximal channel open probability occurs and k is the slope of the curve. The line of best fit yielded $V_{1/2}$ and k values of -9 mV and 5.8 , respectively.

Inactivation: The peak current (I) was normalized relative to the maximal value (I_{max}) obtained at a holding potential (V_h) of -90 mV and plotted against the conditioning pulse potential. Data were fitted by a Boltzmann function according to the following equation: $I/I_{\text{max}} = 1/[1 + \exp(V_{1/2} - V/k)]$ where V is the membrane potential during the pre-pulse, $V_{1/2}$ the potential at which the half-maximal channel inactivation occurs and k the slope of the line. Data are shown for two pre-pulse durations - 4 s (○) and 15 ms (●). The lines of best fit have $V_{1/2}$ and k values of -50 mV and 7.3 (4 s) and of -31 mV and 11.2 (15 ms) respectively. Note the presence of a non-inactivated fraction (approximately 20%) with the shorter pre-pulse.

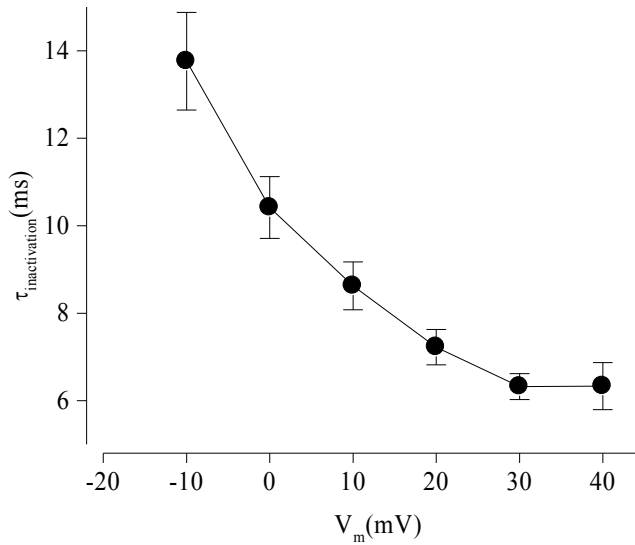


Rates of Inactivation (τ) at Different Potentials:

Differences in the fast inactivation process are also reflected in the rate of channel inactivation (τ) where the recombinant rNav1.8 channel shows a slower rate of inactivation when compared to DRG TTX-R (τ values of 8.6 ± 0.5 and 4.1 ± 0.6 , respectively, at 0 mV). The rate of channel inactivation was voltage dependent, increasing at more positive test potentials (**Figure 4**).

Figure 4. Voltage-dependence of fast inactivation.

The rates of inactivation (τ) at different potentials were determined by fitting the decay phase of the current trace to a single exponential function of the order $A\exp^{-t/\tau} + C$; where A is the current amplitude at the start of the fitting region, t is time and C the steady state asymptote. τ is plotted against test potential (V).

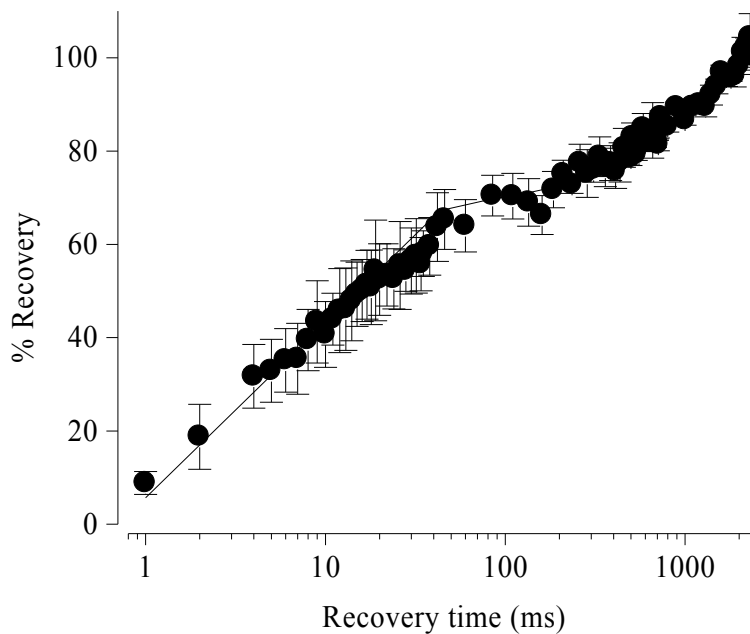


Recovery from Inactivation:

The recovery from inactivation of rNav1.8 was recorded using a repeated two-pulse voltage-clamp protocol that comprised a 50 ms test pulse to 0 mV, followed by a second test pulse to 0 mV. The duration between pulses was increased to measure the rate at which the channel recovered from inactivation following the first pulse. The recovery from inactivation curve was fitted by a bi-exponential function with fast and slow time constants of 12 ± 2 ms ($45 \pm 5\%$ of the total current) and 2271 ± 289 ms ($59 \pm 1\%$ of the total current), respectively (Figure 5, n=3).

Figure 5. Recovery from inactivation.

Currents were activated twice (holding potential -90 mV, test potential 0 mV, 50 ms) with an incremental time delay between the two pulses (recovery time). The peak current evoked by the second pulse (I_2) was normalized relative to the peak evoked by the first pulse (I_1) and plotted against the logarithm of the recovery time. The line of best fit is a double exponential of the form $y = A1*(1-\exp(-t/\tau1)) + A2*(1-\exp(-t/\tau2))$ where t is the time, $\tau1$ and $\tau2$ are the two recovery time constants (13 and 2271 ms respectively) and $A1$ and $A2$ are the relative amplitudes of each exponential (45% and 59% respectively). In all panels, each point represents the mean \pm SEM for at least 3 different cells obtained on at least 3 different experimental days.



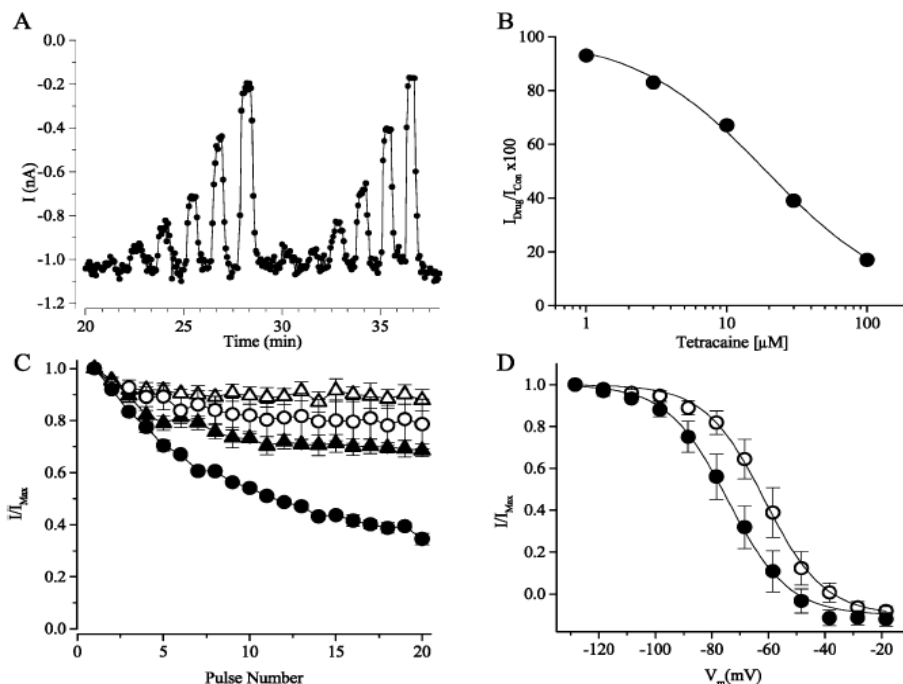
Pharmacology – Tetracaine:

Rat Nav1.8 currents (holding potential -90 mV, test potential 0 mV) steadily increased in amplitude during the first 10 min following whole cell 'breakthrough'. Pharmacological studies were only conducted after this period during which time current amplitude remained highly stable for up to a further 60 min. **Figure 6A** illustrates the stability of these recordings in which it was possible to construct six (two shown) cumulative concentration–response curves to the Na^+ channel blocker tetracaine on a given cell. The dose–response is shown in **Figure 6B**. The geometric mean IC_{50} value for nine cells was 12.5 μM (95% confidence limits 10 – 17 μM).

The blocking effects of tetracaine on rNav1.8 were also studied using the steady-state inactivation paradigm and following repeated rapid channel gating ('frequency dependence paradigm'). Tetracaine (10 μM) produced a significant hyperpolarising shift in the steady-state inactivation curves (4 s pre-pulse) from -60.0 ± 4.9 to -72.6 ± 6.2 mV ($P < 0.01$) with no effect on the slope (values 9.3 ± 0.4 and 10.2 ± 0.2 , respectively; **Figure 6D**). In the repeated gating protocol, the compound block is measured during a rapid train of voltage-clamp pulses that are designed to cycle the rNav1.8 channel through a range of gating states; from closed, through open and inactivated and back to closed. **Figure 6C** illustrates data for tetracaine (3 μM) at stimulus frequencies of 2 and 10 Hz. At each stimulus frequency, tetracaine block is significantly greater at the 20^{th} pulse when compared to the 1^{st} pulse, and this $20:1$ ratio shows a marked dependence on stimulus frequency. The control $20:1$ ratios were 0.88 ± 0.04 (2 Hz) and 0.79 ± 0.1 (10 Hz) and in the presence of tetracaine 0.69 ± 0.02 (2 Hz, $P < 0.01$) and 0.34 ± 0.02 (10 Hz; $P < 0.01$, both $n=4$).

Figure 6. Effects of tetracaine on rNav1.8 channels stably expressed in ND7–23 cells.

- A.** Time course of currents evoked from test pulses (holding potential -90 mV, test potential 0 mV, 50 ms, every 4 s) following repeated addition of increasing concentrations of tetracaine (0.3 – 100 μM). Tetracaine was added via a rapid drug delivery system (lag time 100 ms) until the inhibitory responses reached equilibrium. Note the highly reproducible, responses to tetracaine that were rapidly reversible on washout.
- B.** Mean concentration–response curve to tetracaine. The fitted curve is that of four parameter logistic of the form; $I = (I_{\text{max}} - I_{\text{min}})/(1 + ([\text{Tet}]/\text{IC}_{50})^n) + I_{\text{min}}$, where I is the current in the presence of tetracaine, I_{max} the normalized peak current before drug addition, I_{min} the maximum inhibitory effect, n the Hill slope value, $[\text{Tet}]$ the tetracaine concentration and IC_{50} the tetracaine concentration required to produce 50% current inhibition. The mean IC_{50} value was 12.5 μM and the slope 1.02 .
- C.** Frequency-dependent inhibition by tetracaine. Peak current amplitudes from 20 consecutive pulses (holding potential -90 mV, test potential 0 mV, 20 ms) in the absence (open symbols) and presence (solid symbols) of 3 μM tetracaine at frequencies of 2 Hz (\blacktriangle/\triangle) and 10 Hz (\bullet/\circ). The current is normalized to the first pulse in each case, both in the absence and presence of drug, to account for the tonic (non-use-dependent) drug block. Note the greater blocking effect of tetracaine at higher stimulation frequencies.
- D.** The steady state inactivation curve in the presence (\bullet) and absence (\circ) of 10 μM tetracaine.



IonWorks™ HT assessment of the rNav1.8-ND7-23 cell line:

The rNav1.8-ND7 23 cell line was assessed on IonWorks™ HT. Representative success rates per 384 well plate were as follows. 63% of cells (n=242 cells) sealed and of these, 81% (n=198 cells) had currents above 200 pA. The mean peak current of these cells was 584 ± 94 pA. The cells displayed the slow activation and inactivation kinetics as expected and had a similar I/V relationship as that found using conventional electrophysiology (**Figures 7 and 8**).

Figure 7. Expression of rNav1.8 in ND7–23 cells.

Representative current traces for a step to +20 mV from a holding potential of -90 mV. Time to peak current was 1.6 ± 0.1 ms and the rate of inactivation ($\tau_{\text{inactivation}}$) was 3.3 ± 0.1 ms.

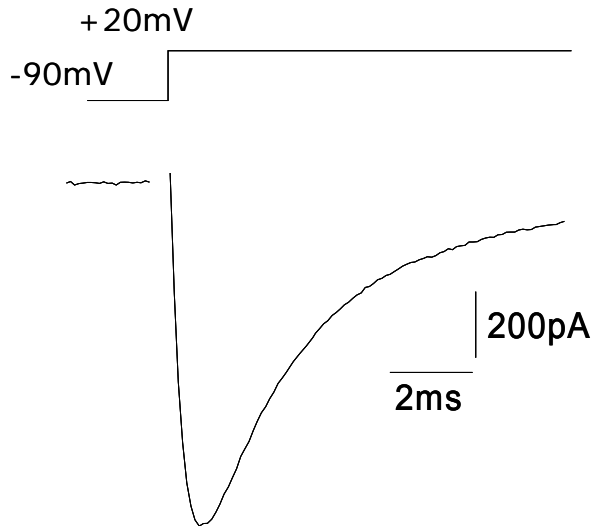
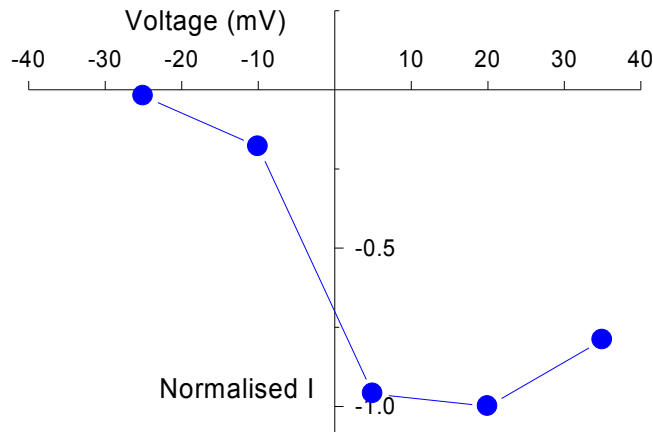


Figure 8. Current/Voltage relationship for rNav1.8 in ND7–23 cells.

The peak current at each test potential was normalised to the maximum current (I/I_{max}).

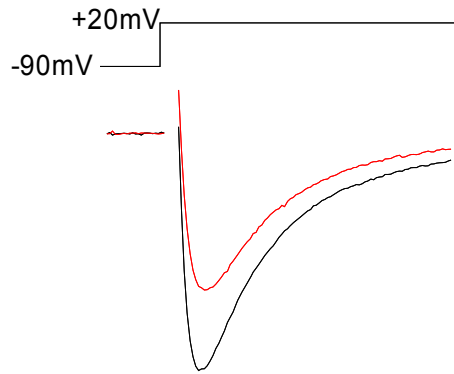


Pharmacology – Tetrodotoxin (TTX) and Tetracaine:

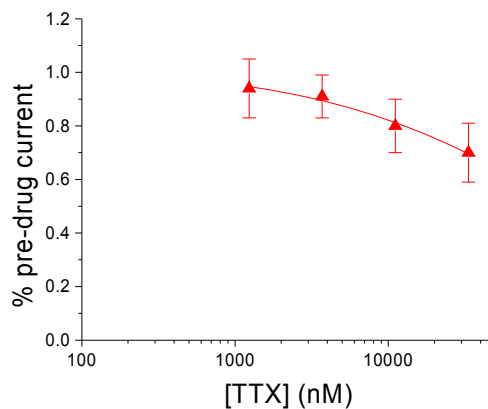
The currents in the rNav1.8-ND7 23 cell line were shown to be largely unaffected by the presence of TTX ($IC_{50} > 30 \mu M$) - **Figure 9A** and **9B** – as expected for a cell line expressing the Nav1.8 channel. In addition, tetracaine was shown to block in the micromolar range – **Figure 9C**.

Figure 9.

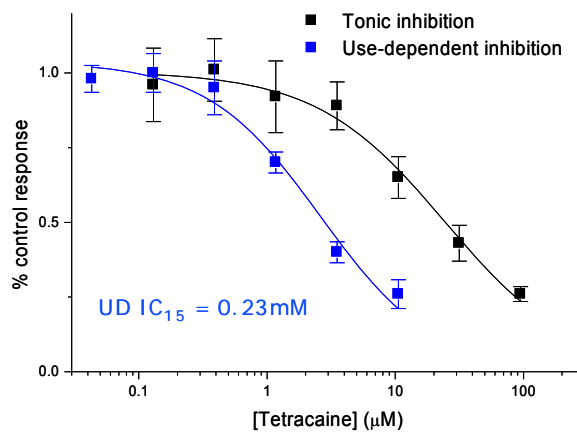
A. Representative current traces in the presence of 33.3 μM (red) or 150 nM (black) TTX.



B. Concentration-response curve for TTX inhibition.



C. Concentration response curves for tetracaine showing a use-dependent mechanism of action. (20 ms pulses were applied at 10 Hz, UD15 is the concentration giving use-dependent block of 15%).

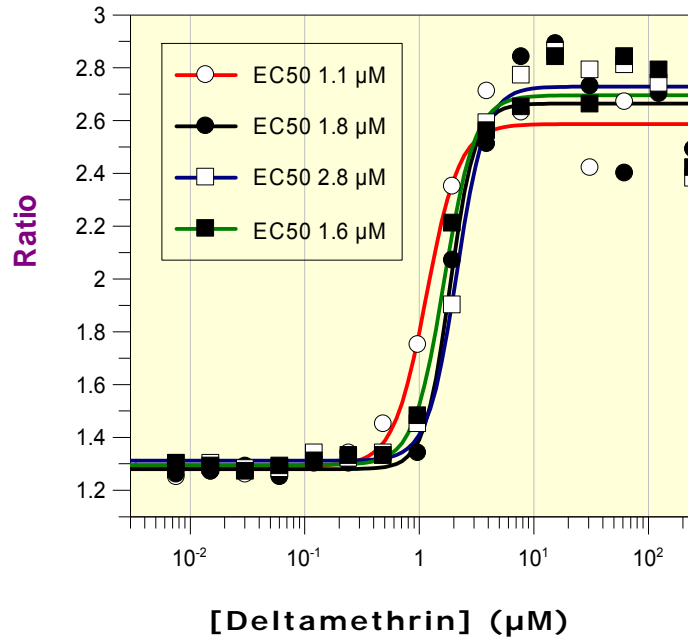


Voltage sensitive probe (VSP) assay (ImageTrak).

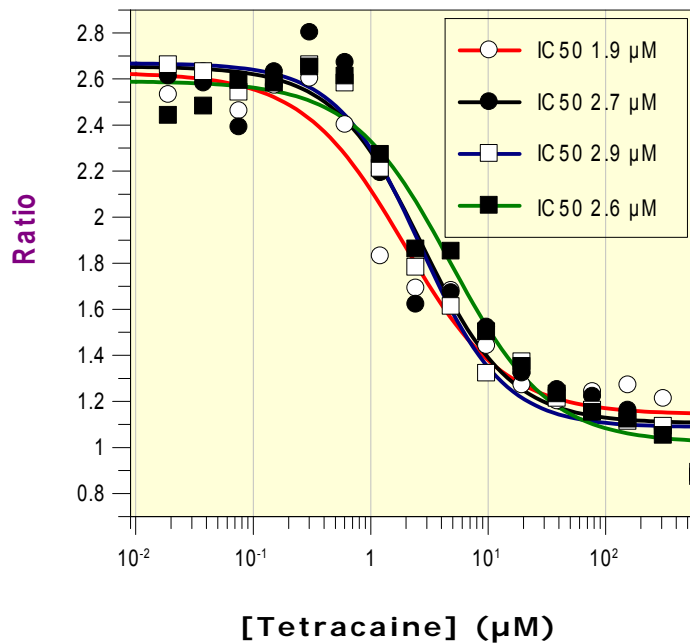
In the presence of voltage sensitive probe fluorescent dyes (VSP) the sodium channel opener, deltamethrin, induced Na⁺-dependent membrane potential depolarizations as indicated by an increase in the relative ratio of fluorescence of the two dyes.

Figure 10.

A. Concentration response curves to deltamethrin.



B. Concentration response curves for the inhibition of the deltamethrin-induced responses by the sodium channel inhibitor tetracaine.



Stability of rNav1.8-ND7-23 Cell Line.

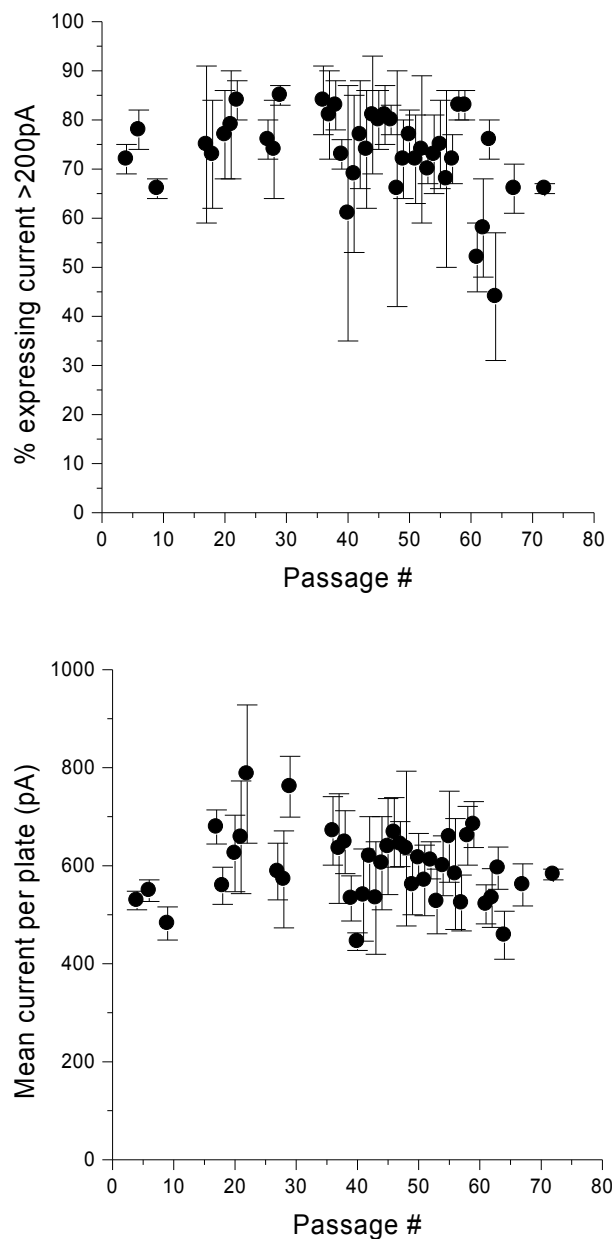
IonWorks™ HT Electrophysiology.

The rNav1.8-ND7-23 cell line has stable expression for >70 passages.

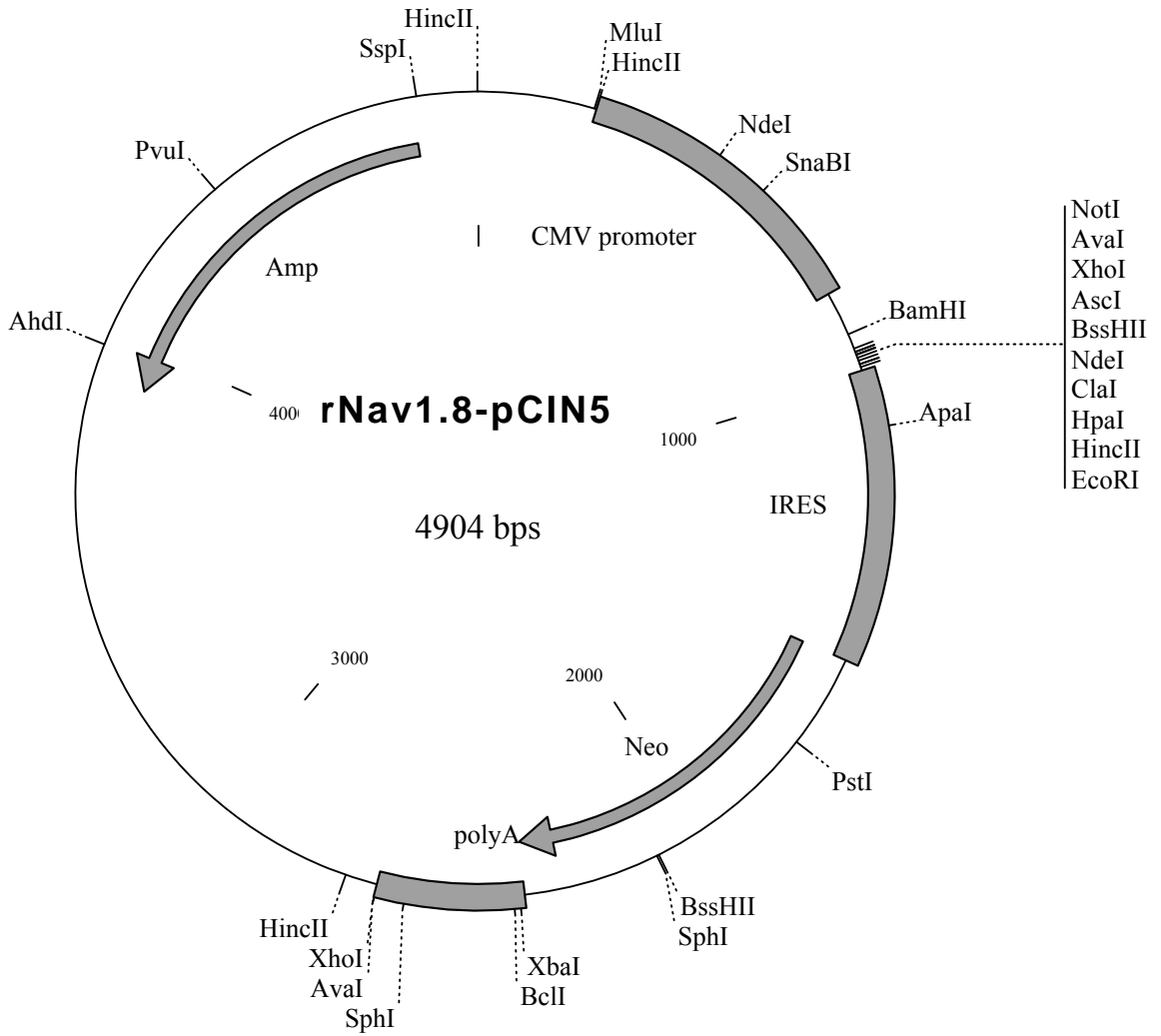
Functional channel expression, defined as cells expressing hERG tail current of ≥ 200 pA, was monitored using IonWorks™ HT. This data and the mean current amplitude are shown in **Figure 11**.

Figure 11. Stability of expression over passage.

The upper panel shows the percentage of cells expressing a mean peak tail current >200 pA at +20 mV from cell passages 4 – 72. The lower panel shows the mean current amplitude per 384-well patch plate (mean \pm SEM).



Vector:



Polylinker: CMV-KpnI-rNav1.8-NotI-XhoI-AscI-ClaI-HpaI-EcoRI-IRES-neo

rNav1.8 Sequence (Accession Number U53833):

References

- Dekker, L.V., Daniels, Z., Hick, C., Elsegood, K., Bowden, S., Szestak, T., Burley, J.R., Southan, A., Cronk, D. and James, I.F. (2005). Analysis of human Nav1.8 expressed in SH-SY5Y neuroblastoma cells. *Eur. J. Pharmacol.* **528**. 52-58.
- John, V.H., Main, M.J., Powell, A.J., Gladwell, Z.M., Hick, C., Sidhu, H.S., Clare, J.J., Tate, S. and Trezise, D.J. (2004). Heterologous expression and functional analysis of rat Nav1.8 (SNS) voltage-gated sodium channels in the dorsal root ganglion neuroblastoma cell line ND7-23. *Neuropharm.* **46**. 425-438.
- Leffler, A., Reiprich, A., Mohapatra, D.P. and Nau, N. (2006). Use-dependent block by lidocaine but not amitriptyline is more pronounced in TTX-resistant Nav1.8 than in TTX-sensitive Na channels. *J. Pharm. Exp. Ther.* *in press*.
- Schroeder, K., Neagle, B., Trezise D.J. and Worley, J. (2003) IonWorks™ HT: a new high-throughput electrophysiology measurement platform. *J. Biomol Screen* **8 (1)**: 50-64.
- Zhou, X., Dong, X-W., Crona, J., Maguire, M. and Priestley, T. (2003). Vinpocetine is a potent blocker of rat Nav1.8 tetrodotoxin-resistant sodium channels. *J. Pharm. Exp. Ther* **306**. 498-504.